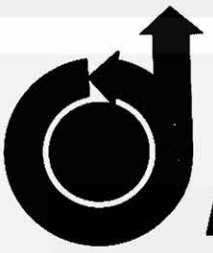

AIAA-81-0386
Microbursts as an Aviation Wind Shear Hazard

T.T. Fujita, University of Chicago, Ill.

AIAA 19th AEROSPACE SCIENCES MEETING

January 12-15, 1981/St. Louis, Missouri

-- NOTES --

MICROBURSTS AS AN AVIATION WIND SHEAR HAZARD

T. Theodore Fujita*
The University of Chicago
Chicago, Illinois

ABSTRACT

Since the Eastern 66 accident in 1975 at JFK International Airport, downburst-related accidents or near-miss cases of jet aircraft have been occurring at the rate of once or twice a year. A microburst with its field, comparable to the length of runways, could induce a wind shear that endangers landing or lift-off aircraft. Latest near-miss landing (go around) of a 727 aircraft at Atlanta, Ga., on 22 August 1979 implied that some microbursts are so small that they may not trigger the warning device of the anemometer network installed and operated at major U.S. airports. A second microburst example, obtained during the NIMROD experiment in the Chicago area on 29 May 1978, is discussed in detail. The nature of microburst and its possible detection by Doppler radar are discussed. Finally, plans for future studies of small-scale microburst phenomena are given.

1 Introduction

Aircraft operations, for both comfort and safety, are closely related to the weather situations along the flight path. High pressure regions (anticyclones) are generally dominated by fine weather, while turbulent weather occurs in or near the frontal zone. Nonetheless, we cannot always generalize these simple relationships irrespective of the scales of atmospheric disturbances.

The high pressure vs. fine weather relationship is no longer valid in mesoscale high-pressure systems, called the "pressure dome" by Byers and Braham (1949). They also defined the "pressure nose" to be a small mesoscale high-pressure spot at the foot of an intense downdraft.

The scale-dependent airflows in frontal zones are summarized in Table 1. Large scale weather systems, highs, lows, and fronts were discovered by Norwegian meteorologists back in the 1920s. Since then mesoscale highs were mapped extensively by the U.S. Thunderstorm Project in 1946 and 1947.

Table 1. Two types of atmospheric disturbances, high pressure and front, which operate in three distinct scales. This table shows that the horizontal scale of air motion alters the disturbance characteristics significantly. In general, the smaller the scale the larger the wind shear.

HIGH PRESSURE SYSTEMS		
Large-scale High (1000 km or larger)	Mesoscale High (10 to 100 km)	Small Mesohigh (less than 10 km)
● Anticyclone ● Diverging wind ● Large-scale subsidence ● Clockwise rotation ● Fine weather	● Pressure dome ● Diverging outflow ● Sinking motion ● Straight-line outflow ● Bad weather	● Pressure nose ● Downburst outflow ● Descending current ● Straight-line outburst ● Rain or virga

FRONTAL ZONES		
Large-scale Front (100 km or longer)	Mesoscale Front (10 to 100 km)	Microscale Front (less than 10 km)
● Warm or cold front ● Converging wind ● Rising motion ● Bad weather	● Gust front ● Converging flow ● Upward current ● Rain or no rain	● Outburst front ● Converging flow ● Upward current ● Rain or dust

*Professor of Meteorology

Gust fronts, one of the most active mesoscale fronts, were studied by Charba (1974), Goff (1975) (1976), and Lee et al. (1978). These studies revealed that gust fronts are characterized by the converging flow and the upward current with or without rain during the frontal passage (Refer to FRONTAL ZONES in Table 1).

The downburst wind, occurring near the foot of a strong downdraft, was first identified by Fujita (1976) and studied further by Fujita and Byers (1977), Fujita and Caracena (1977), Fujita (1978), and Caracena and Maier (1979). These studies indicated that the downburst is characterized by a pressure nose, descending current, straight-line outburst, with rain or virga (Refer to HIGH PRESSURE SYSTEMS in Table 1).

Most researches on gust fronts were initiated and performed by the National Severe Storms Laboratory based intensively on the NSSL tower data, while downburst researches were pursued at the University of Chicago. It should be noted that gust fronts and downbursts are entirely different, both in scales and in their effects upon the penetrating aircraft.

The entire area of an airport will be affected by a passing gust front, while a downburst may affect only a small section of a large airport because of its small dimensions and short life. The point frequency of downbursts is significantly lower than those of gust fronts. This is, probably, why a large number of gust fronts were recorded by the NSSL tower while downburst winds have not been recorded. Furthermore, the characteristics of recorded winds should vary according to the relative location between the tower and the downburst center.

In view of small dimensions and short life, the downburst research at the University of Chicago has been based on (1) the aerial photography and mapping of the downburst damage, and (2) the low-level, short-range scan of Doppler radar of the NIMROD (Northern Illinois Meteorological Research on Downburst) Network.

The purpose of this paper is to define the nature of the diverging and frontal winds in relation to their horizontal scales and to assess the wind shear events likely to be experienced during traverses (Figure 1).

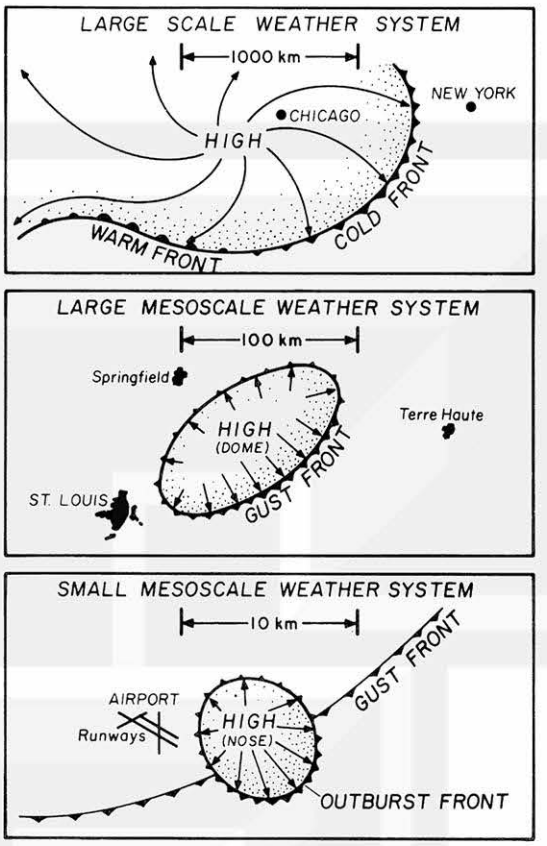

Fig. 1. High pressure areas and associated frontal zones in three different scales. Large scale highs accompany fine weather while mesoscale highs, bad weather.

2. Definition of Wind Shear

The meterological definition of wind shear is the "local variation of the wind vector or any of its components in a given direction", according to the Glossary of Meteorology (1959).

By expressing the wind vector with W and its x, y, and z components with u, v, and w, respectively, we write

$$W = i\,u + j\,v + k\,w \qquad (1)$$

where i, j, and k are unit vectors pointing toward x, y, and z, respectively.

Wind shear which affects a moving object, such as an aircraft, can be expressed by moving the coordinate system with the aircraft, thus referring to the Lagrangian coordinates.

We choose x in the horizontal direction of the ground velocity, G; y, toward the left of the aircraft; and z, upward. Let L be the length measured in the direction of the ground velocity. The variation of wind velocity at the aircraft is given by

$$\frac{\delta W}{\delta t} = G\frac{\partial W}{\partial L} + \frac{\partial W}{\partial t} \qquad (2)$$

where the second term on the right side denotes the local variation of the vector wind caused either by the formation of a new wind system or by an advection of a wind system into the flight path.

Noting that L is a function of x and z, we write

$$\frac{dx}{dL} = \cos\alpha \quad \text{and} \quad \frac{dz}{dL} = \sin\alpha \qquad (3)$$

where α denotes the elevation angle of vector G, which is $\pm$ 3°when an aircraft flies along the glideslope.

Table 2. Extreme values (maxima and minima) and the shear of component winds, u, v, and w at the aircraft flying toward the direction of positive u. The underlined values and shear could cause difficulties in maintaining the nominal flight path.

		u (HEAD OR TAILWIND) (+) TAILWIND	(-) HEADWIND
$\frac{\delta u}{\delta t}$	(+)	Tailwind Increase (Tinc)	Headwind Decrease (Hdec)
	(0)	Maximum Tailwind (Tmax) Minimum Tailwind (Tmin)	Maximum Headwind (Hmax) Minimum Headwind (Hmin)
	(-)	Tailwind Decrease (Tdec)	Headwind Increase (Hinc)

		v (CROSSWIND) (+) CROSSWIND FROM RIGHT	(-) CROSSWIND FROM LEFT
$\frac{\delta v}{\delta t}$	(+)	Right Crosswind Increase (Rinc)	Left Crosswind Increase (Linc)
	(0)	Maximum Right Crosswind (Rmax) Minimum Right Crosswind (Rmin)	Maximum Left Crosswind (Lmax) Minimum Left Crosswind (Lmin)
	(-)	Right Crosswind Decrease (Rdec)	Left Crosswind Decrease (Ldec)

		w (VERTICAL WIND) (+) UPDRAFT	(-) DOWNDRAFT
$\frac{\delta w}{\delta t}$	(+)	Updraft Increase (Uinc)	Downdraft Decrease (Ddec)
	(0)	Maximum Updraft (Umax) Minimum Updraft (Umin)	Maximum Downdraft (Dmax) Minimum Downdraft (Dmin)
	(-)	Updraft Decrease (Udec)	Downdraft Increase (Dinc)

Putting Eqs. (1) and (3) into Eq. (2), we have

$$\frac{\delta W}{\delta t} = i\,A + j\,B + k\,C \qquad (4)$$

where

$$A = \frac{\delta u}{\delta t} = i\left(G\frac{\partial u}{\partial x}\cos\alpha + G\frac{\partial u}{\partial z}\sin\alpha + \frac{\partial u}{\partial t}\right) \qquad (5)$$

$$B = \frac{\delta v}{\delta t} = j\left(G\frac{\partial v}{\partial x}\cos\alpha + G\frac{\partial v}{\partial z}\sin\alpha + \frac{\partial v}{\partial t}\right) \qquad (6)$$

$$C = \frac{\delta z}{\delta t} = k\left(G\frac{\partial w}{\partial x}\cos\alpha + G\frac{\partial w}{\partial z}\sin\alpha + \frac{\partial w}{\partial t}\right) \qquad (7)$$

Terms A, B, and C denote the variation of tailwind, crosswind, and vertical wind, respectively.

Quantities u, v, w, and A, B, C, can be either positive, zero, or negative, resulting in the 18 types of wind shear presented in Table 2. Of these, the underlined events could cause the loss of altitude when they are excessive either individually or when combined.

3. Gust Front

Gust front is the frontal zone of advancing cold air characterized by a sudden increase in the windspeed followed by gusty winds. The source of the cold air with strong gusts is predominantly thunderstorms which frequently form a squall line.

During the penetration of a typical gust front in Figure 2, tailwind changes into headwind regardless of the direction of the traverse. The rate of the tailwind increase and the headwind decrease is generally small, occurring during the approach and receding phases of the traverse.

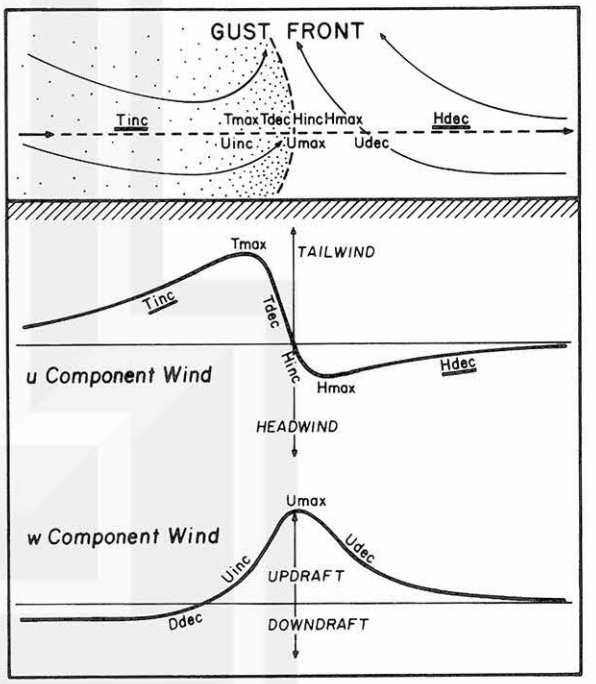

Fig. 2. Wind-shear events expected to occur during a traverse through a gust front.

At or near the frontal boundary, tailwind changes into headwind very rapidly. Vertical winds encountered are mostly upward unless an aircraft flies through a roll cloud (or roll) which may exist near a gust front.

4. Downburst

The term "downburst" was first used by Fujita (1976) in his analysis of the Eastern 66 accident in 1975 at JFK International Airport. It was defined as "A localized, intense downdraft with vertical current exceeding a downward speed of 12 fps or 720 fpm at 300 ft above the surface." This downward speed is comparable to the rate of descent of a jet aircraft during its final approach.

Fig. 3. Three stages of downburst phenomenon. The descending stage (top), contact stage (middle), and outburst stage (below).

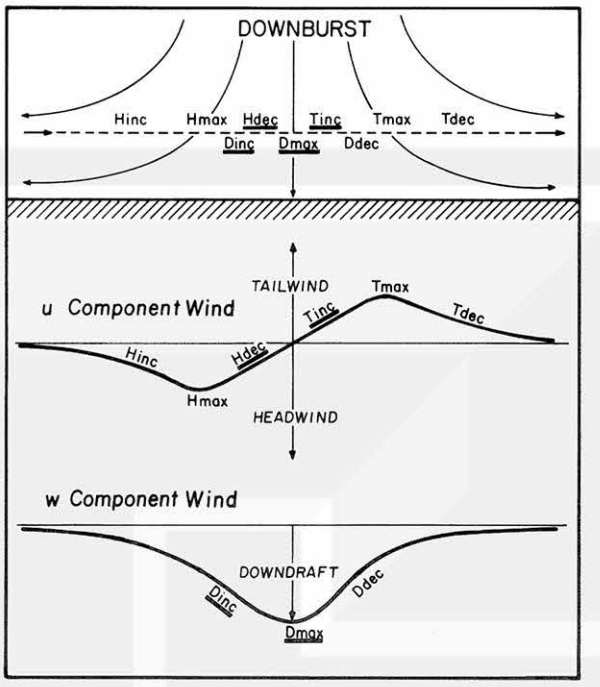

Fig. 4. Wind-shear events expected to occur during a traverse through a downburst.

Subsequent studies showed that downbursts descend with precipitation which sometimes evaporates as "virga" before reaching the ground. Three photographs in Figure 3 show three stages of the downburst,which are descending, contact, and outburst stages. It should be noted that the downward current turns into an outburst current as it hits the surface.

An aircraft which traverses a downburst near the surface could lose its altitude due to the low-level wind shear.

A schematic drawing (Figure 4) presents a low-level traverse from left to right. If an aircraft flies through the center of a downburst, it will not be affected by the crosswind. Of a number of events experienced by the aircraft, increase of downdraft (Dinc), decrease of headwind (Hdec), maximum downdraft (Dmax), and increase of tailwind (Tinc), contribute to the loss of altitude. Dangerously, however, all of these events occur one after another or simultaneously resulting in a significant sinking which may or may not be arrested for a successful fly out.

Downburst is accompanied by changes in vector winds in a small area, which could affect aircraft operations seriously. The basic rule of the events is "the smaller the scale, the faster the time variations." Therefore, the wind systems comparable to glidepaths or runways are the inducer of dangerous wind shear.

4. Microburst

The horizontal dimensions of mesoscale disturbances commonly referred to in meteorology are 10 to 100 km. Squall lines, gust fronts, and large thunderstorms are examples of mesoscale weather systems.

Studies since the JFK accident in 1965 revealed that the typical scale of downbursts is between 1 and 10 km. Refer to Fujita and Byers (1977), and Fujita and Caracena (1977).

Because the scales of violent storms, such as tornadoes and some downbursts, are much smaller than mesoscale, Fujita (1979) proposed a violent-storm related scale. The misoscale (read as my-so-scale) was assigned the dimensions of 100 to 1000 m. Mesoscale and misoscale are divided artificially by the square root of 10 or 3.16 km (approximately 10,000 ft).

Now the microburst is defined as the "misoscale downburst", the extent of which is comparable to the lengths of runways (Figure 5).

On June 24, 1975, two Eastern flights were affected by two separate microbursts. Eastern 902 flew through on the right side of a microburst, experiencing right drift and serious wind shear (Figure 6).

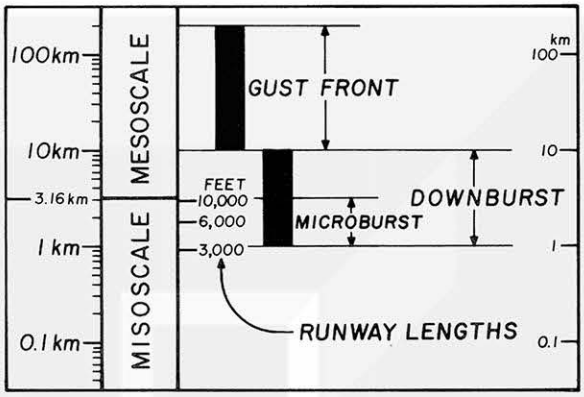

Fig. 5. Scales of gust front and downburst. Misoscale (read as my-so-scale) downburst is called microburst.

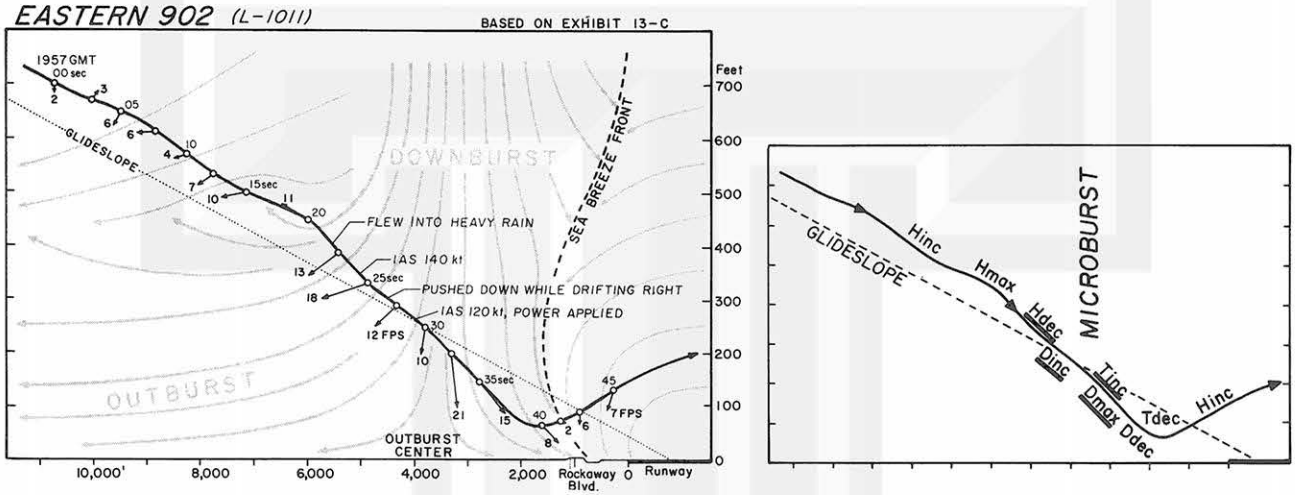

Fig. 6. Flight path of Eastern 902 on June 24, 1975, at JFK airport. Wind-shear events are shown in the right side figure.

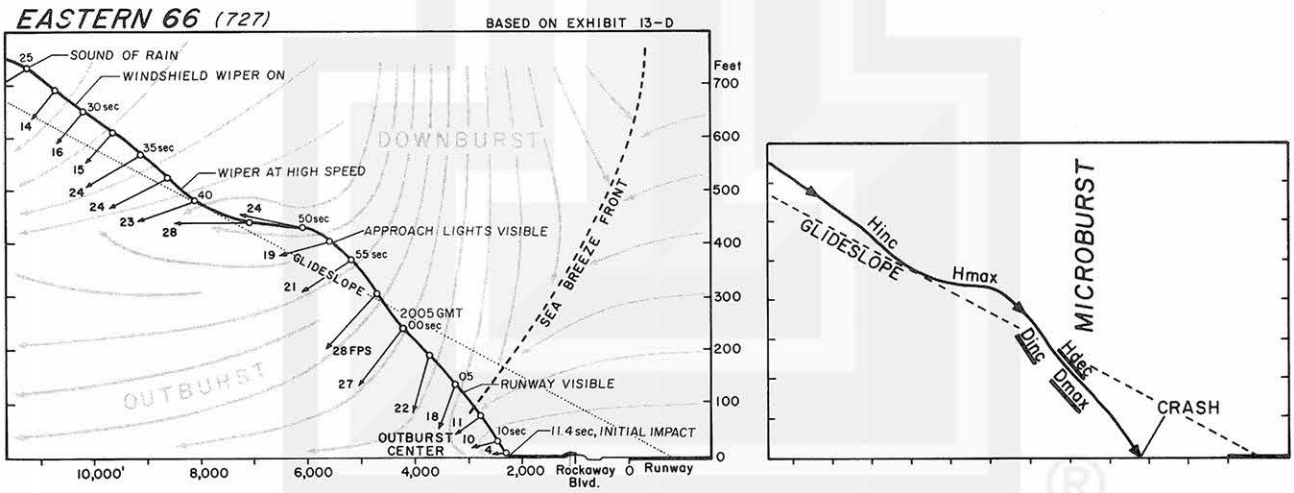

Fig. 7. Flight path of Eastern 66 on June 24, 1975, at JFK airport. Wind-shear events are shown in the right side of the figure.

Eastern 66 flew through the center of the second microburst. Headwind decrease (Hdec) coupled with the maximum downdraft (Dmax) was so severe that it crashed 2,400 ft short of the runway threshold (Figure 7).

On August 22, 1979, the low-level wind shear alert system at Atlanta Airport did not trigger an alert. On its final approach to 27L, Eastern 693 encountered a strong downflow which could be caused by a microburst in its contact stage (Figures 8 and 9).

Fig. 8. Distribution of the LLWSAS anemometers at Atlanta Airport as of August 22, 1979.

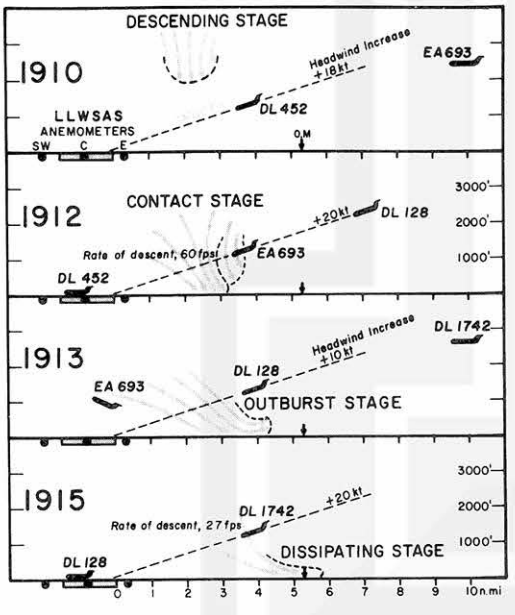

Fig. 9. Aircraft locations in relation to a microburst which descended between the outer marker and runway 27L Between 1910 and 1915 GMT, August 22, 1979.

5. Warm-sector Microburst

When a microburst descends toward the ground, the condition of the low-level atmosphere affects the airflow characteristics of the descending air.

Stationary Microburst

A schematic view in Figure 10 depicts the three stages of a microburst which keeps descending over one particular spot on the earth. At first the downflow air deflects horizontally at high speed during the outburst stage.

As the cold air accumulates beneath the microburst, the cushion of cold air prevents the successive downflow from hitting the ground to spread violently. During this cushion stage, the extreme winds weaken and microburst becomes less dangerous.

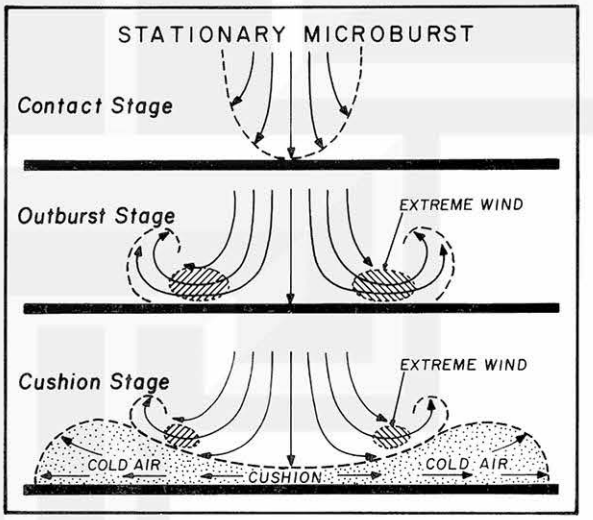

Fig. 10. Three stages of a stationary microburst.

Traveling Microburst

When a microburst travels, the descending current does not descend on to the cushion of the cold air. Instead, the successive downflow descend on to the ground ahead of the cold air. Meanwhile, the cold air, being left behind, acts like a slide, which deflects the downflow into a slanted flow (Figure 11).

A traveling microburst on May 29, 1978, was depicted by a Doppler radar of NIMROD (Northern Illinois Meteorological Research On Downburst). Against our initial expectation, the height of the maximum wind was extremely low, less than 50 m above the ground.

Figure 12 denotes the Doppler radar measured u-component windspeed with its peak, 32 m/sec or 62 kts. This peak wind was located 1300 m or 4300 ft ahead of the center of the downflow.

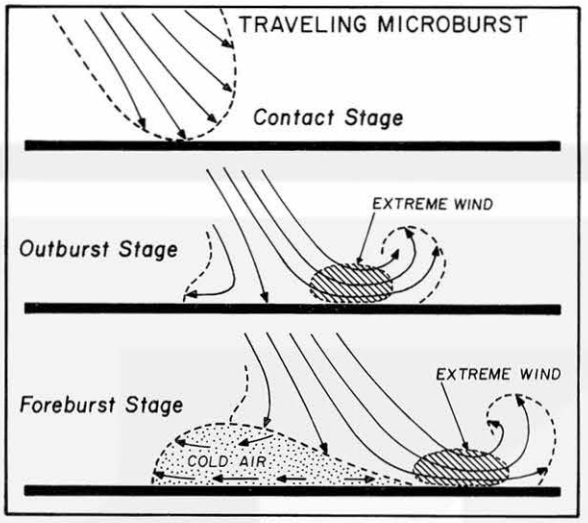

Fig. 11. Three stages of a traveling microburst.

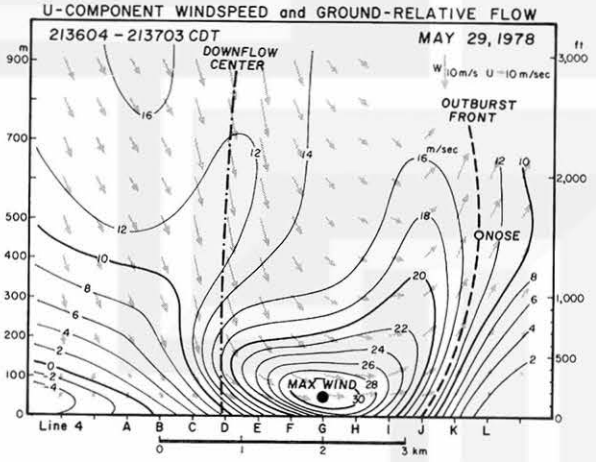

Fig. 12. Vertical cross section of u-component windspeed of the May 29, 1978 microburst obtained by the Yorkville Doppler radar in the NIMROD Network.

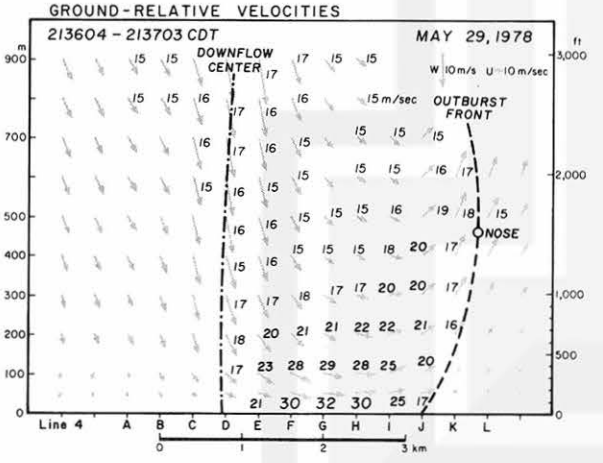

Fig. 13. Vertical cross section of the total windspeed of the microburst in Fig. 12. The maximum windspeed of 32 m/s is seen 1.3 km ahead of the downflow center at 50 m AGL. Windspeed decreases toward the outburst front.

Wind velocities in the vertical plane (Figure 13) reveal that the downflow speed of 17 m/sec at 900 m above the ground increased into 32 m/sec horizontal flow at 50 m (or less) above the ground. Such an acceleration was resulted by the squeezed outflow layer above the ground ahead of the cold air.

6. Cold-sector Microburst

Cold-sector microbursts descend behind cold fronts or gust fronts where the surface is covered with cold air.

Figure 14 shows an example of the cold-sector microburst which occurred near the O'Hare International Airport after the passage of a gust front. The gust front was more than 100 km long accompanied by the warm-sector winds from south-westerly directions. Temperature to the north of the gust front was 5°to 7°C colder.

The microburst descended through the cushion of cold air causing an abrupt increase

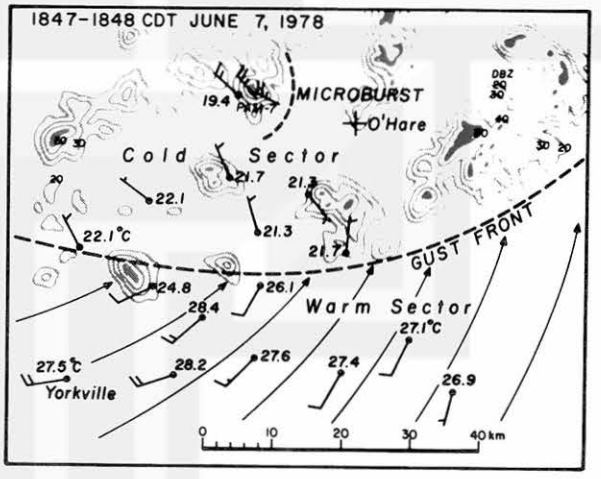

Fig. 14. A cold-srctor microburst detected 15 km to the west of the O'Hare International Airport by the NIMROD Doppler radar at O'Hare.

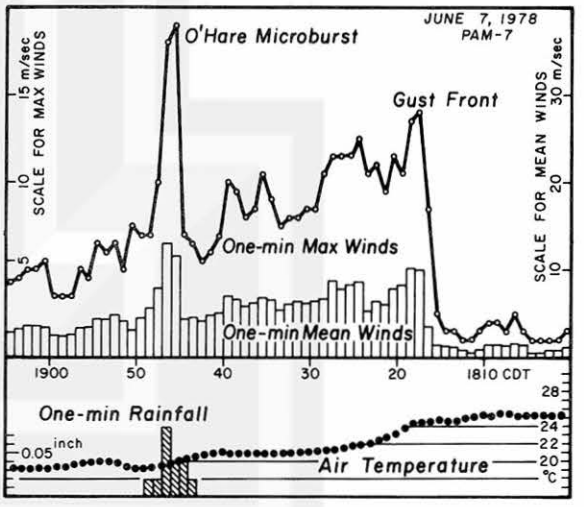

Fig. 15. Wind variation at PAM station No. 7 recorded during the passage of both gust front and microburst in Fig. 14

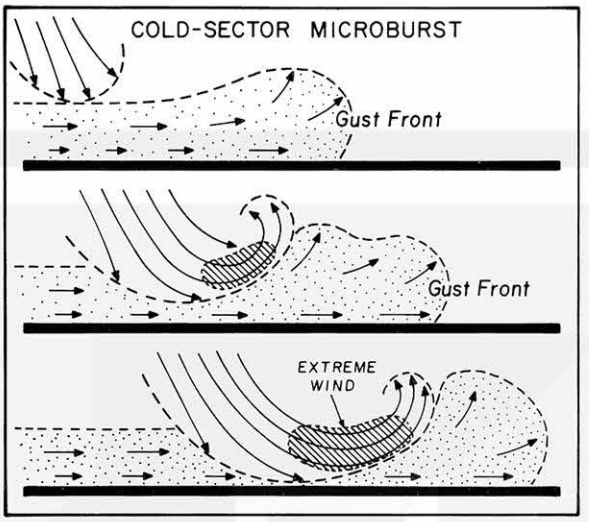

Fig. 16. Schematical cross sections of a cold sector microburst as it sinks into the cold air behind a gust front.

in the windspeed measured by the anemometer of PAM station No. 7. The station was affected by two disturbances; first, by the gust front (mesoscale) and second, by the microburst (miso-scale). The gust-front wind showed an abrupt increase followed by a gradual decrease while the microburst wind lasted only two minutes with its 38 kt peak speed.

The cold-sector microburst must sink into the cold air before reaching the surface. The descending current will first make contact with the top of the cold air moving toward the gust front. Then it interacts with the cold air, pushing forward and downward (Figure 16).

During the mature stage, a pocket of the extreme wind will be located above the cushion of the cold air. The vertical wind shear, vertical gradient of horizontal wind, beneath the pocket of the extreme wind is so large that surface anemometers may not register the extreme wind aloft.

Doppler radar measurements of the micro-burst in Figures 14 and 15 revealed that the extreme wind of 22 m/sec (43 kt) was located 250 m (820 ft) above the ground while a surface anemometer was measuring only 4 to 5 m/sec (8 to 10 kt) winds.

Schematic penetration of two aircraft, the one descending and the other ascending along the 3 glidepaths are presented in Figure 17. Both aircraft will experience a headwind increase (Hinc) followed by a dangerous headwind decrease (Hdec). Finally, the aircraft will fly through the region of the maximum downdraft (Dmax) 1 m/s to 5 m/s in the downflow speeds. Since the rate of descent and that of ascent are approximately 3 m/s, a combination of the wind-shear events could result in a serious difficulty in maintaining the altitude.

It should be emphasized that the surface anemometer recorded the peak windspeed of 13 m/s four minutes after the passage of the extreme wind aloft.

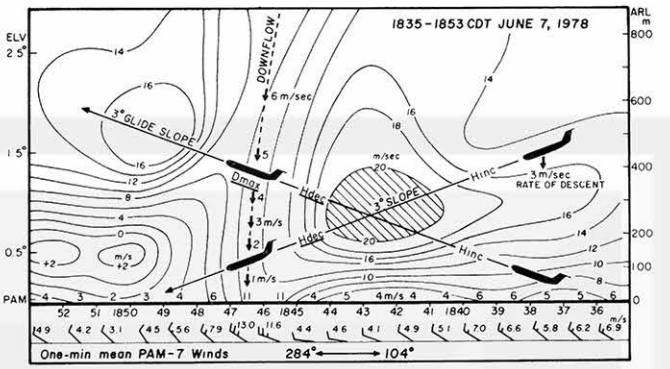

Fig. 17. Two hypothetical traverses through the center of the microburst in Fig. 14 and 15. The u-component wind-speeds were obtained by the NIMROD radar at O'Hare

The foregoing example suggests strongly that a ground-based network, no matter how extensive and dense their station distribution may be, will probably fail to detect the extreme winds of the cold-sector microburst. The high winds on the ground (Fig. 17) occur where the downflow hits the ground, away from the location of the extreme winds aloft.

7. Detection of Microbursts by Doppler Radar

Examples of wind systems presented in this paper indicate clearly that the microburst is the inducer of the wind shear which causes the loss of altitude at low levels.

A network of surface anemometers are very effective in depicting advancing gust fronts for warning purposes. It is unlikely, however, that microbursts can be detected by anemometers in time for alerting pilots to take proper actions.

The short-lived, small scale microburst can be detected by one Doppler radar once we know the downburst signatures at various altitudes. The heights of the maximum wind are estimated to be 10 to 50 m (30 to 100 ft) AGL for warm-sector microbursts and 100 to 300 m (300 to 1000 ft) AGL for cold-sector micro-bursts.

It is essential to conduct a basic-research experiment in an around a major airport to obtain Doppler signatures of all types of microbursts.

Figure 18 describes the distribution of Doppler radars and surface anemometers for conducting such an experiment. Five location identified with letters M_1 through M_5 are where microburst-related incidents occurred in and around the five major airports at JFK, Denver, Tucson, Philadelphia, and Atlanta during the past five years.

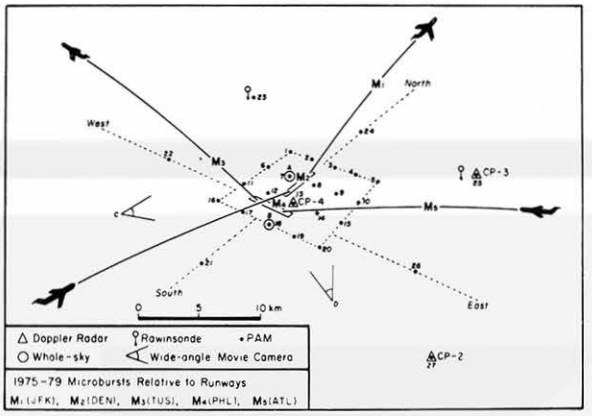

Fig. 18. A schematic view of a network for obtaining the signatures of microburst. A Doppler radar (CP-4) is placed in the airport ground to perform 360-deg scans for detecting winds along the glide slopes. The second Doppler (CP-3) and the third one (CP-2) will provide us with the data for performing dual and triple Doppler analyses. Doppler-measured winds are compared with the surface winds measured by 27 PAM statinons placed in and around the airport.

8. Conclusions

Both gust fronts and microbursts are the inducers of the low-level wind shear which endangers aircraft operations during the landing and takeoff phases.

Nevertheless, these two types of disturbances are quite different from each other in terms of their airflow structure. Gust front is a mesoscale frontal zone while a downburst accompanies a mesoscale high-pressure area.

A gust front can be detected efficiently by a network of ground-based anemometers, while microbursts can hardly be detected by anemometers in time for an effective warning. However, a single Doppler radar with proper display systems will be capable of monitoring both gust fronts and microbursts within 25 to 30 km range of an airport.

In order to advance the basic knowledge of the microburst phenomenon, aiming toward the design of a fool-proof detection system, it is necessary to operate a fact-finding network of Doppler radar and ground-based anemometers.

Acknowledgements

This research has been supported by grants from NSF/ATM 79-21260, NOAA/NESS NA80AA-D-00001, and NASA NGR 14-001-008.

References

Byers, H.R. and R.R. Braham Jr. (1949), The Thunderstorm. U.S. Government Printing Office, Washington D.C., 287 pp.

Caracena, F. and M. Maier (1979) Analysis of a microburst in the FACE meteorological mesonetwork. Preprints, Eleventh Conf. on Severe Local Storms, Kansas City, Amer. Meteor. Soc., 279-286.

Charba, J.P. (1974) Application of gravity current model to analysis of squall-line gust front, Mon. Wea. Rev., 102, 140-156.

Fujita, T.T. (1976) Spearhead echo and downburst near the approach end of a John F. Kennedy Airport runway, New York City. SMRP Res. Paper No. 137, University of Chicago, 51 pp.

Fujita, T.T. (1978) Manual of downburst identification. SMRP Res. Paper No. 156, University of Chicago, 104 pp. NTIS PB-286048.

Fujita, T.T. (1979) Objectives, operation, and results of Project NIMROD. Preprints, Eleventh Conf. on Severe Local Storms, Kansas City, Amer. Meteor. Soc., 259-266.

Fujita, T.T. and H.R. Byers (1977) Spearhead echo and downburst in the crash of an airliner. Mon. Wea. Rev., 105, 129-146.

Fujita, T.T. and F. Caracena (1977) An analysis of three weather-related aircraft accidents. Bull. Amer. Meteor. Soc., 58, 1164-1181.

Goff, R.C. (1975) Thunderstorm outflow kinematics and dynamics. NOAA Technical Memorandum, ERL NSSL 75, 63 pp.

Goff, R.C. (1976) Vertical structure of thunderstorm outflows, Mon. Wea. Rev., 104, 1429-1440.

Glossary of Meteorology (1959) Amer. Meteor. Soc., 638 pp.

Lee, J.T., J. Stokes, Y. Sasaki, and T. Baxter (1978) Thunderstorm gust fronts - observations and modeling, FAA-RD-78-145, 116 pp.

-- NOTES --